Effects of Compositional Variations on CO2 Foam Under Miscible Conditions

Kahrobaei, Siavash; Li, K; Vincent-Bonnieu, Sebastien; Farajzadeh, Rouhi

DOI
10.3997/2214-4609.201701793

Publication date
2017

Document Version
Final published version

Published in
IOR NORWAY 2017

Stavanger NORWAY
The National IOR Centre of Norway
EAGE

We B15

Effects of Compositional Variations on CO2 Foam Under Miscible Conditions

S. Kahrobaei* (Delft University of Technology), K. Li (Delft University of Technology), S. Vincent Bonnieu (Shell Global Solutions International) & R. Farajzadeh (Shell Global Solutions International)

SUMMARY

Foam can potentially solve the associated problems with gas injection by reducing the mobility of the injected gas leading to a more stable displacement front. It is known that under immiscible conditions, the presence of oil can be detrimental for foam stability through several mechanisms. Under miscible conditions, there is no separate oil or gas phase; instead, CO2 and oil mix in different proportions forming a phase with varying composition at the proximity of the displacement front. There are then two fundamental questions, which arise from addition of surfactant to the system: (1) what is the nature of the "mixed phase" in the presence of the surfactant, and (2) how do the properties of this mixture change with compositional variations? This study reports the results of core-flood experiments conducted using CO2 and decane (nC10) as the model oil under miscible conditions. Surfactant and a mixture of CO2-decane were co-injected with variations of CO2 molar fractions, mixture volume fractions and total flow rates. We found that separate injection of CO2 or oil with the surfactant solution into the cores creates in-situ fluids that exhibit both low-quality (increasing viscosity with decreasing fraction of surfactant) and high-quality (decreasing viscosity with decreasing fraction of surfactant) regimes. However, upon simultaneous injection of CO2 and oil with the surfactant solution and depending on the molar fraction of CO2 in CO2-decane mixture (xCO2), three distinct regimes were observed. In Regime 1 (xCO2>0.8) the apparent viscosity of the in-situ fluid was the highest and increased with increasing xCO2. In Regime 2 (xCO2<2) the apparent viscosity increased with decreasing xCO2. In Regime 3 (0.2< xCO2<0.8) the apparent viscosity of the fluid remained relatively low and insensitive to the value of xCO2. Shear-thinning rheology was observed in all three regimes: supercritical CO2 foam (xCO2 =1), decane emulsion (xCO2 = 0), as well as CO2-decane-surfactant floods. Moreover, in Regime 1 and Regime 2, there is a transition at shear rates from 10 s-1 to 100 s-1, where the apparent viscosity increases by one order of magnitude. In Regime 3, however, this transition is not observed. Finally, we found that the current implicit-texture foam model cannot simulate our experimental data.

1. Introduction

Gas is an ideal injection fluid for enhancing oil recovery because of its good displacement efficiency (resulting in a low residual-oil saturation) as well as its high injectivity (allowing for large injection rates for a certain drawdown pressure). When the pressure is above a certain pressure referred to as the minimum-miscibility pressure (MMP) the displacement efficiency of the gas can be as high as unity because of the elimination of the interfacial tension (IFT) or capillary forces (Correa et al., 1990; Dindoruk and Firoozabadi, 1996; Verlaan and Boerrigter, 2006; Kahrobaei et al., 2012; Ameri et al., 2013). Nevertheless, in field applications the ultimate recovery of a (miscible) gas-injection process can still remain low because of the inefficient volumetric sweep, which is the overall result of viscous fingering, gravity override, and gas channeling (Farajzadeh et al., 2012). Foaming the injected gas can potentially overcome these shortcomings by reducing gas mobility and thus sustaining a more stable displacement front (Farajzadeh et al., 2009; Andrianov et al., 2012; Farajzadeh et al., 2012). A major "challenge" in application of foam is the detrimental effect of oil on the generation and stability of foam (Bergeron et al., 1993; Schramm, 1994; Andrianov et al., 2012; Farajzadeh et al., 2012). There is a consensus that when the oil saturation in a porous medium is above a limiting range foam starts to collapse or its generation slows down (Friedmann and Jensen, 1986; Yang and Reed, 1989; Hudgins and Chung, 1990; Law et al., 1992; Schramm, 1994). Many studies regarding foam-oil interaction have focused on the bulk and porous-media experiments with distinctive oil and gas phases, i.e., the results are more relevant for immiscible-displacement processes. However, under miscible conditions the effect of oil on foam is different because of the absence of separate oil and gas phases. Instead, gas and oil form a single phase with different compositions, which is because of the extraction of the light and the heavy components of the oil by the injected gas or due to the mixing caused by local variations of the permeability. Consequently, a transition zone is formed, which separates the injected gas from the reservoir oil. Ultimately, under miscible conditions, when the flood pressure is high enough, the transition zone would be a single phase of gas and oil (Holm and Josendal, 1974). The miscible mixture of oil and gas at the displacement front is called "mixed-phase" throughout this study.

In case a surfactant solution is available, lamellae separating bubbles, i.e. foam, are created inside the pores. In the high-pressure floods, the dense state of the gas acts more like a liquid than like the gas but it does not cause any difficulty in the formation of the foam (Heller, 1994; Chabert et al., 2016). Suffridge et al. (1989) and Mannhardt et al. (1996) also showed the possibility of foam formation in porous media with hydrocarbon gas under miscible conditions. It should be noted that "foams" are mainly referred to the dispersion of the gas in a liquid phase; whereas, the dispersions of a dense, liquid-like state of the gas phase or solvent in an aqueous phase might more appropriately be called emulsions (Mannhardt et al., 1996). However, for the sake of simplicity the "foams/emulsions" generated with the supercritical CO_2 are referred to as foams in this paper.

The compositional variations near the displacement front during miscible floods are expected to affect the foam rheology, which might in turn impact the performance of the mobility-control process. The nature of the foam flow regimes and their rheological behavior is the focus of the current study. In particular, we aim at understanding the effect of the changes in the composition of the gas phase on the foam behavior during miscible-displacement processes. This is achieved by performing series of experiments in which different fractions of CO_2, oil, and a surfactant solution are co-injected into a porous medium.

The structure of the paper is as follows. First, the experimental setup and procedure are described in Section 2. Section 3 provides the results of the foam-quality-scan and shear-thinning experiments and explains the implications of our results on the efficiency of the miscible displacement. Finally the paper ends with some concluding remarks.

2. Experiments

2.1. Experimental Methodology

Two types of experiments were performed to study the effect of compositional variation of the front on CO_2 foam behavior. In the first series of the experiments, the so-called foam-quality scans (Ma et al., 2013; Ma et al., 2014) were conducted to investigate the in-situ rheology of the mixture of the surfactant solution and the "mixed phase" under steady-state conditions. In the second series of the experiments, the flowrate-dependency of the rheology of the in-situ formed fluids was examined.

In both types of experiments the gas and liquid phases are injected simultaneously until the steady state pressure is measured. The measured pressure drop is an indicator of the resistance against the flow of the residing fluid. In this study the measured steady-state pressure drops are converted into apparent viscosity of flowing phase, using single-phase Darcy's law:

$$\mu_{app} = \frac{kA}{q_m + q_l}\frac{|\Delta p|}{L}, \tag{1}$$

where k [m^2] is the absolute permeability, A [m^2] is the cross-sectional area, q_m [m^3/s] and q_s [m^3/s] represent the flowrates of the mixed-phase and the surfactant solution, respectively, and Δp [Pa] is the pressure drop along the length of L [m]. Moreover, the fractional flow of the mixed phase or mixed-phase quality (fm) is defined by,

$$f_m = \frac{q_m}{q_m + q_s}. \tag{2}$$

The error bars for each data point were calculated from the standard deviation of the steady-state-pressure measurements.

2.2. Chemicals and Materials

Alpha Olefin Sulfonate (AOS) $C_{14\text{-}16}$ (Stepan® BIO-TERGE AS-40 KSB) was used as the surfactant with an active concentration of 0.50 wt% (~ 0.04 M). The properties of the foam films stabilized by this surfactant can be found in Farajzadeh et al. (2008). The NaCl concentration was fixed to 1.0 wt% (~ 0.17 M) in all experiments. The critical micelle concentration (CMC) of the surfactant in demineralized water with 1 wt% of NaCl was measured as 0.008 wt% (~ 6.27×10-5 M) using the Du Noüy ring method. Decane (nC_{10}) and Carbon Dioxide (CO_2) were used as the model oil and the gas, respectively. The properties of CO_2 and C10 at our experimental conditions are reported in Table 1. Six 17-cm cylindrical quasi-homogenous Bentheimer sandstone cores with a diameter of 3.8 cm were used as the porous medium for six different CO_2-C_{10} compositions. The permeability of these cores varied between 1600 to 2000 mD. The average porosity of the cores was 0.23. The cores were coated with a thin layer of high temperature resistant glue and placed inside a cylindrical core holder.

Table 1 *Fluid properties at 90 bar and 40 °C.*

Fluid	Density [kg/m^3]	Viscosity [cP]
CO_2	485.50	3.48×10^{-2}
nC_{10}	722.38	7.66×10^{-1}

2.3. Experimental Conditions

Numerical and experimental studies were performed to determine the minimum-miscibility pressure (MMP) of CO_2 and C_{10}. The numerical PVT simulations were performed using PVTSim simulation package (Calsep, 2017) and the Peng-Robinson equation of state (Peng and Robinson, 1976). **Figure 1a** shows the phase envelopes for the mixtures with different CO_2-C_{10} molar fractions. To achieve full miscibility between the gas and the oil, the experiments were conducted at 90 bar and 40 °C, denoted with an orange star on the figure, which is located in the single-phase region for all CO_2-C_{10} molar fractions. To further assure that the selected experimental pressure is above the MMP of the CO_2-

decane system, seven core-flooding experiments were conducted. In these experiments CO_2 was injected into the cores fully saturated with decane at the constant temperature of 40 ºC. The recovery factors (defined as the amount of the produced oil divided by the oil initially in the core) of these experiments after two pore volumes of CO_2 injection are shown in **Figure 1b**. The oil recovery factor increases with the increasing pressure until 83 bar. Above this pressure, the recovery factor does not change significantly with the increasing pressure, which indicates that the MMP is 83 bar at 40 ºC. The less-than-unity recovery factor can be attributed to the instabilities (viscous fingering) and bypassing of the oil because of the large viscosity difference between CO_2 and decane under the experimental conditions.

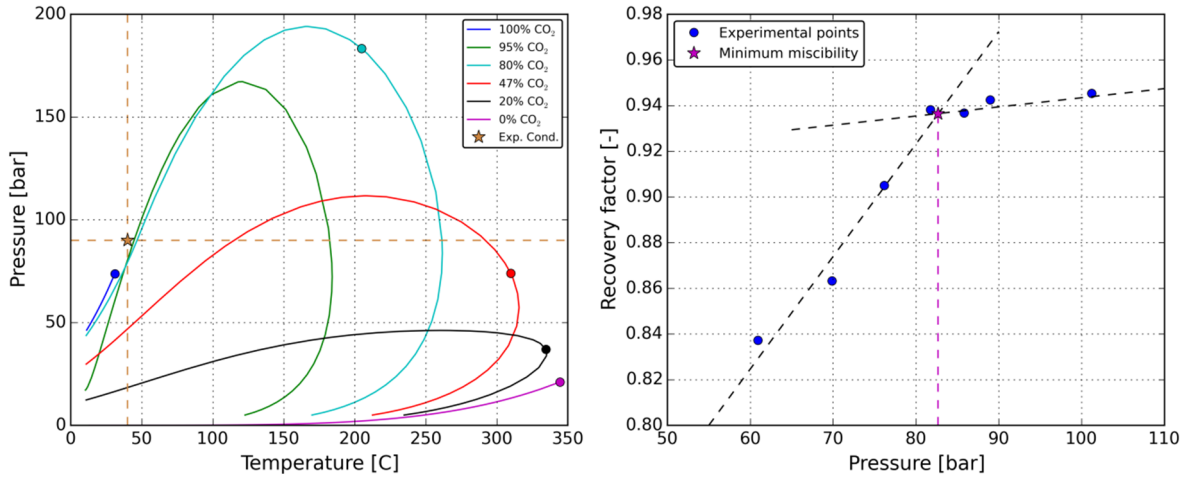

Figure 1 *(a) The phase diagram of the CO_2-decane binary system, calculated by PVTSim simulation package and the Peng-Robinson equation of state. (b) Recovery factors of decane after injection of two pore volumes of CO_2 under different experiments pressures at the constant temperature of 40 °C.*

2.4. Experimental Setup

The schematic of the experimental apparatus is shown in **Figure 2**. The experimental setup consisted of an injection unit, a test unit, a pressure-controlling unit and a data acquisition unit. The injection unit contained three Quizix TM QX-6000 pumps to supply CO_2, decane and the surfactant solution at constant rates. A spiral tubing was added to the CO_2-C_{10} injection line to ensure complete mixing of CO_2 and C_{10} before the core inlet. The core-holder was placed vertically in an oven to maintain the temperature at 40 °C. The overall pressure difference along the core was measured using a differential pressure transducer connected to the input and the output lines of the core-holder. Two back-pressure regulators (BPR) in series were connected at the outlet of the core to maintain the system pressure at 90 bar and to mitigate the pressure fluctuations in the system. The accuracy of the pressure transducers were 1 mbar.

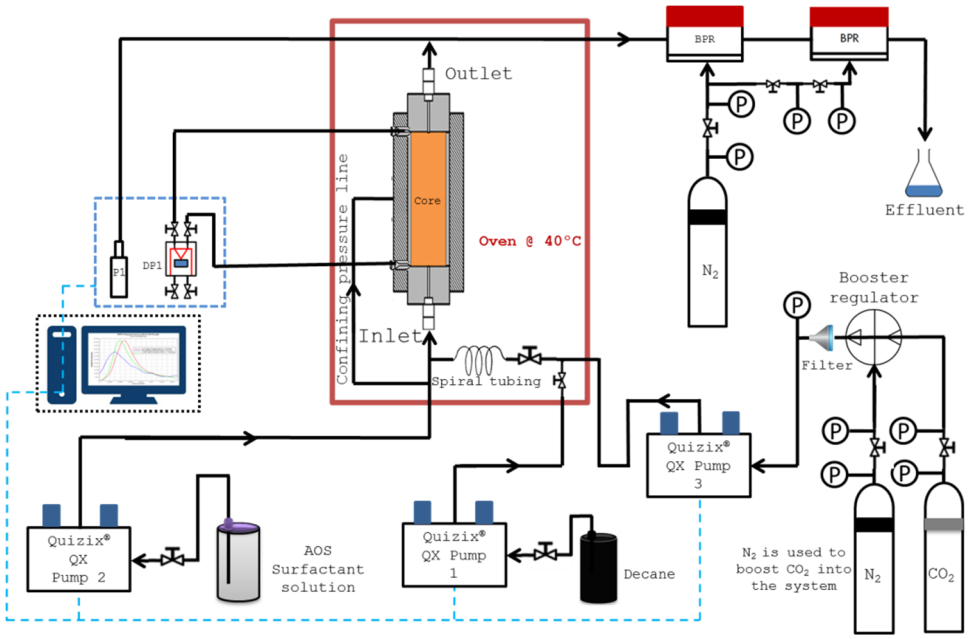

Figure 2 *Schematic of the experimental apparatus.*

2.5. Experimental Procedure

2.5.1. Foam-quality-scan experiments

After assuring that the setup was leak free, the air was removed from the cores by injecting CO_2. CO_2 is more soluble in water and can be easily removed by injecting brine at elevated pressures. Once the gas was removed, the permeability of the core was calculated by measuring the pressure drop along the core at different brine flowrates using Darcy's law. Subsequently, the cores were pre-saturated with the surfactant solution to satisfy the rock adsorption. In the foam-quality scans, the mixed-phase (a mixture of CO_2 and decane) was co-injected with the AOS surfactant solution at different volume fractions (qualities) into the core to generate foam inside the core. For all qualities, the mixed-phase and the surfactant solution were co-injected with a constant total flowrate of 1.60 ml/min corresponding to a total superficial velocity of 6.66 ft/day. The co-injection was continued until the steady-state pressure (within the accuracy of our measurements) was obtained. Subsequently, the quality was altered and the system was allowed to reach a new steady state. In this set of experiments, six different molar fractions of CO_2 (x_{CO2}) and decane (x_{C10}) were used with randomly-ordered mixed-phase qualities. Note that the composition of the mixed-phase was controlled by adjusting CO2 and C_{10} volume rates using two separate pumps. Moreover, in this paper "mixed-phase", represented by f_m, refers to the mixture of CO_2 and decane under miscible conditions. **Table 2** provides a summary of the foam-quality-scan experiments. Note that foam becomes coarser as the permeability of the core decreases because of the increase in the limiting capillary pressure (Farajzadeh et al., 2015). However, the permeabilities of the cores used in our experiments are in the same range and therefore significant impact on foam behavior is not expected.

Table 2 *Summary of the quality-scan experiments.*

Experiment No.	Permeability [mD]	CO_2 molar fraction in CO_2-C_{10} mixture [-]
1	2056	1
2	2059	0.95
3	1946	0.8
4	1741	0.47
5	2090	0.2
6	1606	0

2.5.2. Shear-thinning experiments

In this set of experiments, the total flow rate of the mixed-phase and the surfactant solution was varied in increasing steps while the mixed-phase quality was kept constant. The experiments started with a total flow rate of 0.20 ml/min (~ 0.82 ft/day). After reaching the steady-state pressure profile, the total flow rate was then increased to reach a new steady state. The total flow rate was ultimately increased up to 5 ml/min (~ 20.69 ft/day). All experiments were conducted at the mixed-phase quality of 0.60. **Table 3** summarizes the shear-thinning experiments.

Table 3 *Summary of the sear-thinning experiments.*

Experiment No.	Permeability [mD]	CO_2 molar fraction in CO_2-C_{10} mixture [-]
1	2059	0.95
2	1946	0.8
3	1741	0.47
4	2090	0.2
5	1606	0

3. Results and Discussions

3.1. Foam-quality-scan experiments

In this set of experiments, six different molar fractions of decane and CO_2 were used to investigate the effects of the compositional variations on the foam-flow behavior under miscible conditions.

It is well-known that in the absence of oil, two flow regimes can be inferred from the steady-state foam scan experiments (with a constant total rate): the low-quality regime and the high-quality regime. In the low-quality regime, the pressure gradient (or apparent viscosity) increases with increasing gas fractional flow (or foam quality) whereas in the high-quality regime, the pressure gradient decreases with the increasing gas fractional flow (Ma et al., 2013; Ma et al., 2014). Foam behavior in the low-quality regime depends on the bubble trapping and release and the gas velocity influences the pressure gradient (Rossen and Wang, 1999; Alvarez et al., 2001). In the high-quality regime the foam behavior is dominated by coalescence governed by the limiting capillary pressure and the pressure gradient is influenced by the liquid velocity (Khatib et al., 1988; Kam et al., 2007; Farajzadeh et al., 2015).

Figure 3a shows the pressure gradient along the cores as a function of the mixed-phase quality (fractional flows of the mixed-phase) with different molar fractions of CO_2. The corresponding apparent viscosities of the flowing phase, calculated from Eq. (1), are also shown in **Figure 3b**.

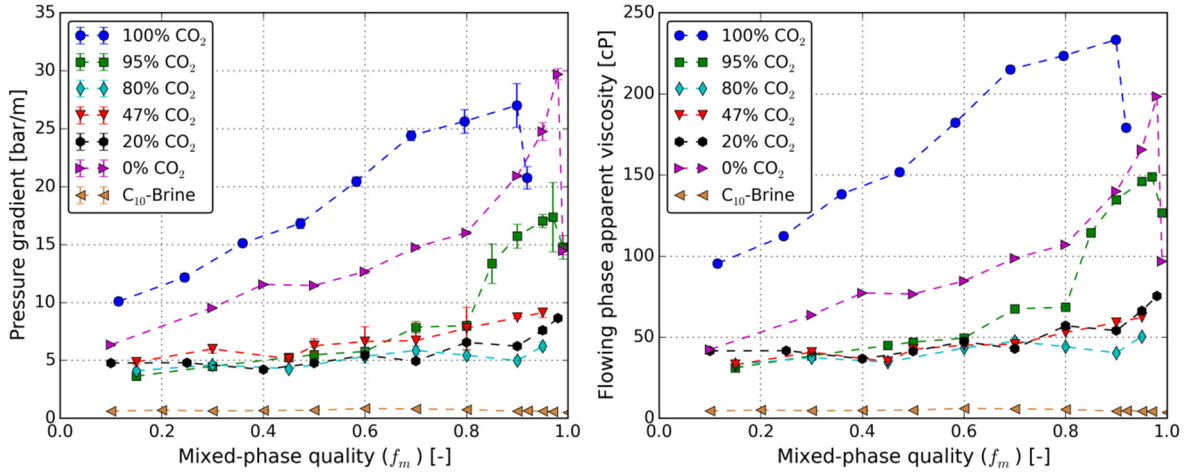

Figure 3 *(a) the pressure gradient along the core and (b) the calculated apparent viscosity of flowing phase at different mixed-phase quality with different compositions of CO_2.*

It appears from Figure 3 that variation in the composition of the mixed-phase greatly impacts the in-situ rheology of foam in porous media. Similar to the immiscible foam experiments (Eftekhari et al., 2015; Zeng et al., 2016), for the experiments with 100% CO_2 (blue curve) and 100% C_{10} (purple curve) two separate rheological regimes are observed. In these two cases the apparent viscosity of the flowing phase increases with the increasing fractional flow of the non-aqueous phase (low-quality regime) until it reaches a maximum at the transition quality (f_m^{tr}) and decreases afterwards (high-quality regime). The transition quality (f_m^{tr}) for the supercritical CO_2 foam is around 0.90 and for C_{10} emulsion is around 0.97. The maximum apparent viscosity for the supercritical CO_2 foam and the C10 emulsion are 240 cP and 200 cP, respectively. For both cases, in both low- and high-quality regimes, fluids (foam/emulsion) with large apparent viscosities are observed. Nevertheless, the apparent viscosity of CO_2 foam is almost two times larger than the apparent viscosity of the C_{10} emulsion in most fractional flows of the non-aqueous phase. The experimental results of the co-injection of C_{10} and brine in the absence of surfactant are added to Figure 3 for the sake of comparison (dark orange curve). The pressure gradient at all fractional flows of C_{10} is around 0.11 bar/m. The corresponding apparent viscosity of the flowing phase is 4.5 cP.

For the case of x_{CO2} = 0.95 (green curve), at the mixed-phase qualities between 0.1 and 0.8, the apparent viscosity of the flowing phase does not change significantly and remains almost constant at about 50 cP. However, at the mixed-phase quality of 0.80, there is a rapid increase in the apparent viscosity of the flowing phase. Furthermore, between the mixed-phase qualities of 0.8 and 0.97, there is an increase in the apparent viscosity of the flowing phase with the increase in the mixed-phase quality. Finally, between mixed-phase qualities of 0.97 and 1 the apparent viscosity of the flowing phase decreases. This indicates that even a small addition of decane can decrease the foam apparent viscosity compared to the pure CO_2.

For the cases with intermediate CO_2 molar fractions ($0.2 \leq x_{CO2} \leq 0.8$) the apparent viscosity of the flowing phase is almost constant (around 50 cP) at all mixed-phase qualities.

The relatively high apparent viscosities of the flowing phase (>50 cP) for all mixture compositions show that under miscible conditions, CO_2 foam can still have a good mobility control in the presence of the oil. Moreover, it is important to note that for the molar fractions between $0.2 \leq x_{CO2} \leq 0.8$ (under our experimental conditions) no distinguishable separate rheological regimes are observed, which is the basis of the current foam simulators. This indicates that for example the implicit-texture (IT) foam

model, i.e., that of STARS (CMG, 2010; Farajzadeh et al., 2012; Ma et al., 2014), cannot be used to model the behavior observed in our experiments.

Figure 4 plots the calculated apparent viscosity of the flowing phase as a function of the CO_2 molar fraction. It can be seen in Figure 4 that for a fixed quality, the case with 100% CO_2 (x_{CO2} = 1) exhibits the highest steady-state flowing-phase apparent viscosity, followed by the cases with x_{CO2} = 0 and x_{CO2} = 0.95. Figure 4 also reveals that for the mixtures with CO_2 molar fractions between $0.2 \leq x_{CO2} \leq 0.8$, the steady-state apparent viscosity of the flowing phase remains unchanged with varying mixed-phase composition.

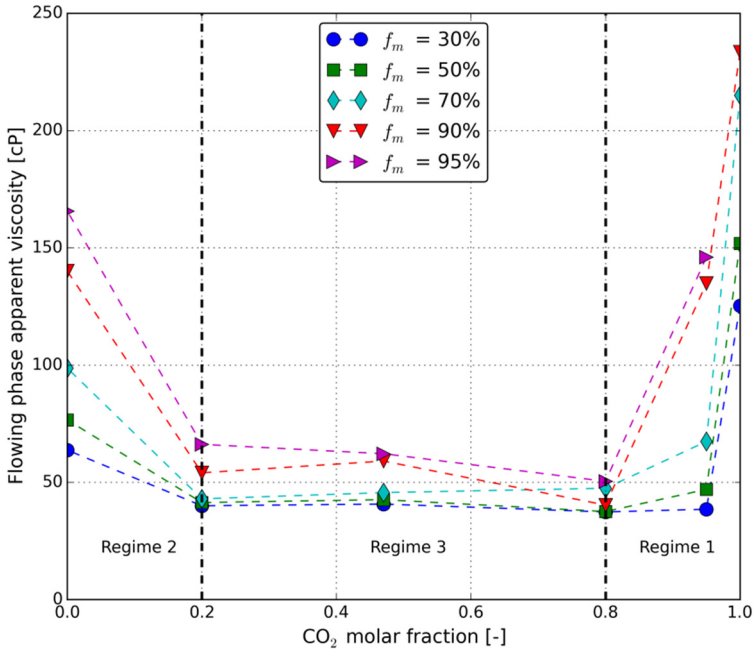

Figure 4 *Apparent viscosity of flowing phase versus CO_2 molar fraction (x_{CO2}), at different mixed-phase qualities. Black dashed line indicates three different regimes based on the compositional variations effects on CO_2 foam.*

Consequently, three different regimes can be defined based on the effects of the mixed-phase composition on CO_2 foam-flow behavior:

- **Regime 1 (x_{CO2}>0.8):** this regime represents the CO_2-rich region, with a high apparent viscosity;
- **Regime 2 (x_{CO2}<0.2):** this regime represents the decane-rich region with a relatively high apparent viscosity;
- **Regime 3 ($0.2 \leq x_{CO2} \leq 0.8$):** this regime represents the intermediate molar fractions of CO_2 with an apparent viscosity that is nearly invariant with the fractional flow of the mixed phase.

Although we do not have direct measurements, the transition from regime 1 (CO_2-rich floods) to regime 2 (decane-rich floods) through regime 3 can be seen as a transition from a "foam-like" behavior to an "emulsion-like" behavior.

3.2. Shear-Thinning Experiments

An important characteristic of foam and emulsion is their non-Newtonian shear-thinning behavior, i.e. their viscosity decreases by increasing the shear rates. For foam flow in porous media, in the low-quality regime the apparent viscosity of the foam decreases with increasing shear rates because of the bubble trapping and release and therefore exhibits shear-thinning behavior (Mannhardt et al., 1996; Xiao et al., 2016). A similar behavior has also been reported for emulsions (Herzhaft et al., 2002; Yu et al., 2012). However, the effect of compositional variations of the front on foam rheology, especially in regime 3 ($0.2 \leq x_{CO2} \leq 0.8$), is not fully investigated. Therefore, in this study several shear-thinning

experiments were conducted using different molar fractions of CO_2 and decane to study this phenomenon.

Figure 5 shows the apparent viscosity of the flowing phase as a function of the total velocity (mixed-phase velocity + the surfactant solution velocity) at a constant mixed-phase quality. Results show that there is a transition from a low to a high apparent viscosity of flowing phase in regime 1 (x_{CO2} = 0.95) and regime 2 (x_{CO2} = 0). This transition can be also observed at x_{CO2} =0.8. However, this transition is not observed in regime 3 (x_{CO2} = 0.47, x_{CO2} = 0.2). In regime 3, the apparent viscosity is significantly high (up to 560 cP) at a low velocity (0.82 ft/day). From a practical point of view, this high apparent viscosity at this low velocity can be unfavorable because it can damage the injectivity. This may result in low injection rates for a certain drawdown pressure (Romero et al., 1996; Farajzadeh et al., 2016). In general, all molar compositional fractions of miscible CO_2-C_{10} mixture exhibit shear-thinning behavior, because the apparent viscosity decreases by increasing the velocity. Moreover, it can be seen that all mixed-phase compositions have the same apparent viscosity at higher velocities, which is in line with our findings from foam-quality-scan experiments.

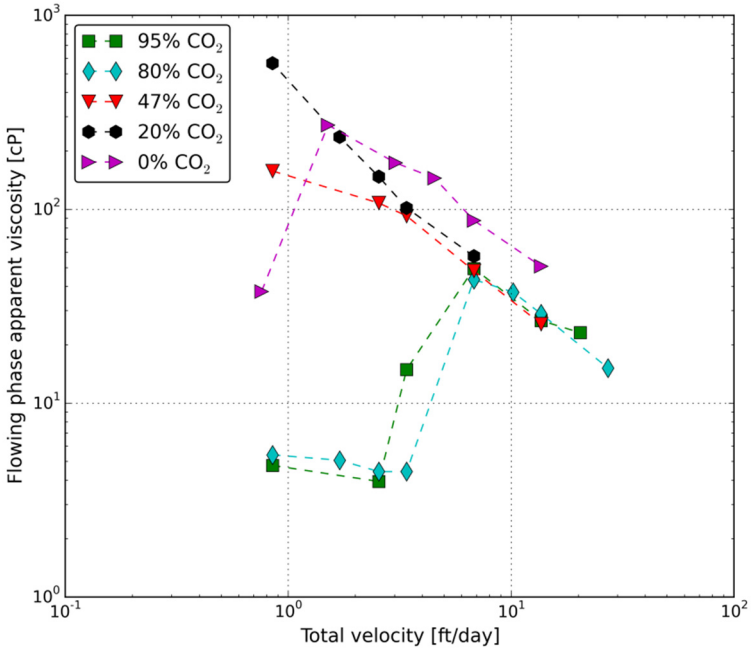

Figure 5 *Apparent viscosity of flowing phase as a function of velocity for different molar fractions of the CO_2-C_{10} system at a constant fractional flow of the mixed-phase.*

4. Conclusions

In this study, through several CO_2-decane-surfactant core-flooding experiments under miscible conditions (90 bar and 40°C), the effects of compositional variations on supercritical CO_2 foam were investigated. For the cases investigated in this study, following conclusions are made:

- Under miscible conditions, CO_2 foam can show good mobility-control in the presence of flowing oil.
- Three different regimes can be defined based on the effects of the mixed-phase compositions on CO_2 foam-flow behavior:
  - Regime 1 (CO_2-rich floods, x_{CO2}>0.8), with a high apparent viscosity (~ 150 to 250 cP);
  - Regime 2 (decane-rich floods, x_{CO2}<0.2), with a relatively high apparent viscosity (~ 50 to 150 cP);
  - Regime 3 (CO_2-decane-surfactant floods, 0.2≤ x_{CO2}≤0.8), with an apparent viscosity that is nearly invariant with the mixed-phase quality and the mixed-phase composition (~ 50 cP).

- All these three regimes exhibit shear-thinning behavior.
- In regime 3, the compositional variations of the displacement front do not significantly affect the apparent viscosity of the flowing phase.
- For the intermediate CO_2 molar fractions, no distinguishable separate rheological regimes are observed and the apparent viscosity of the flowing phase is almost independent of the mixed-phase quality.

5. References

Alvarez, J. M., Rivas, H. J., Rossen, W. R. 2001. Unified Model for Steady-State Foam Behavior at High and Low Foam Qualities. 10.2118/74141-PA.

Ameri, A., Farajzadeh, R., Suicmez, V., Verlaan, M., Bruining, J. 2013. Effect of Non-equilibrium Gas Injection on the Performance of (Immiscible and Miscible) Gas–Oil Gravity Drainage in Naturally Fractured Reservoirs. *Energy & Fuels* **27** (10): 6055-6067. DOI: 10.1021/ef401372d.

Andrianov, A., Farajzadeh, R., Mahmoodi Nick, M., Talanana, M., Zitha, P. L. 2012. Immiscible foam for enhancing oil recovery: bulk and porous media experiments. *Ind. Eng. Chem. Res* **51** (5): 2214-2226. DOI: 10.1021/ie201872v.

Bergeron, V., Fagan, M., Radke, C. 1993. Generalized entering coefficients: a criterion for foam stability against oil in porous media. *Langmuir* **9** (7): 1704-1713 DOI: 10.2172/10192744.

PVTsim 3 Method Documentation, 2017. Lyngby, Denmark., Calsep A/S.

Chabert, M., Cuenca, A., Lacombe, E., Chevallier, E., Nabzar, L., Batot, G. 2016. A Novel Fast-Track Methodology to Evaluate CO2 Foamers Performances. Paper presented at SPE Improved Oil Recovery Conference, 11-13 April, Tulsa, Oklahoma, USA. DOI: 10.2118/179632-MS.

CMG, C. M. G. L. 2010. *STARS User's Guide*. Calgary, Alberta, Canada, Computer Modelling Group Ltd (Reprint).

Correa, A. C., Pande, K. K., Ramey, H. J., Jr., Brigham, W. E. 1990. Computation and Interpretation of Miscible Displacement Performance in Heterogeneous Porous Media. *SPERE* **5** (01). DOI: 10.2118/16704-PA.

Dindoruk, B., Firoozabadi, A. 1996. Crossflow in Fractured/Layered Media Incorporating Gravity, Viscous, and Phase Behavior Effects: Part II-Features in Fractured Media. Paper presented at SPE/DOE Improved Oil Recovery Symposium, 21-24 April, Tulsa, USA. DOI: 10.2118/35458-MS.

Eftekhari, A. A., Krastev, R., Farajzadeh, R. 2015. Foam Stabilized by Fly Ash Nanoparticles for Enhancing Oil Recovery. *Industrial & Engineering Chemistry Research* **54** (50): 12482-12491. DOI: 10.1021/acs.iecr.5b03955.

Farajzadeh, R., Andrianov, A., Krastev, R., Hirasaki, G., Rossen, W. R. 2012. Foam–oil interaction in porous media: Implications for foam assisted enhanced oil recovery. *Adv. Colloid Interface Sci.* **183**: 1-13. DOI: 10.1016/j.cis.2012.07.002.

Farajzadeh, R., Andrianov, A., Zitha, P. 2009. Investigation of immiscible and miscible foam for enhancing oil recovery. *Ind. Eng. Chem. Res* **49** (4): 1910-1919. DOI: 10.1021/ie901109d.

Farajzadeh, R., Eftekhari, A. A., Hajibeygi, H., Kahrobaei, S., van der Meer, J. M., Vincent-Bonnieu, S., Rossen, W. R. 2016. Simulation of instabilities and fingering in surfactant alternating gas (SAG) foam enhanced oil recovery. *Journal of Natural Gas Science and Engineering* **34**: 1191-1204. DOI: 10.1016/j.jngse.2016.08.008.

Farajzadeh, R., Krastev, R., Zitha, P. 2008. Foam films stabilized with alpha olefin sulfonate (AOS). *Colloids and Surfaces A: Physicochemical and Engineering Aspects* **324** (1): 35-40. DOI: 10.1016/j.colsurfa.2008.03.024.

Farajzadeh, R., Lotfollahi, M., Eftekhari, A., Rossen, W., Hirasaki, G. 2015. Effect of permeability on implicit-texture foam model parameters and the limiting capillary pressure. *Energy & fuels* **29** (5): 3011-3018. DOI: 10.1021/acs.energyfuels.5b00248.

Friedmann, F., Jensen, J. A. 1986. Some Parameters Influencing the Formation and Propagation of Foams in Porous Media. Paper presented at SPE California Regional Meeting, 2-4 April, California. DOI: 10.2118/15087-MS.

Heller, J. P. 1994. CO2 Foams in Enhanced Oil Recovery. In *Foams: Fundamentals and Applications in the Petroleum Industry*, Chap. 5, 201-234. Advances in Chemistry, American Chemical Society. DOI: 10.1021/ba-1994-0242.ch005.

Herzhaft, B., Rousseau, L., Neau, L., Moan, M., Bossard, F. 2002. Influence of Temperature and Clays/Emulsion Microstructure on Oil-Based Mud Low Shear Rate Rheology. Paper presented at SPE Annual Technical Conference and Exhibition, 29 September-2 October, San Antonio, Texas. DOI: 10.2118/77818-MS.

Holm, L. W., Josendal, V. A. 1974. Mechanisms of Oil Displacement By Carbon Dioxide. *Journal of Petroleum Technology* **26** (12): 1.427 - 1.438. DOI: 10.2118/4736-PA.

Hudgins, D. A., Chung, T. H. 1990. Long-Distance Propagation of Foams. Paper presented at SPE/DOE Enhanced Oil Recovery Symposium, 22-25 April, Tulsa, Oklahoma. DOI: 10.2118/20196-MS.

Kahrobaei, S., Farajzadeh, R., Suicmez, V. S., Bruining, J. 2012. Gravity-enhanced transfer between fracture and matrix in solvent-based enhanced oil recovery. *Ind. Eng. Chem. Res* **51** (44): 14555-14565. DOI: 10.1021/ie3014499.

Kam, S. I., Nguyen, Q. P., Li, Q., Rossen, W. R. 2007. Dynamic simulations with an improved model for foam generation. *SPE Journal* **12** (01): 35-48

Khatib, Z. I., Hirasaki, G. J., Falls, A. H. 1988. Effects of Capillary Pressure on Coalescence and Phase Mobilities in Foams Flowing Through Porous Media. *SPERE* **3** (03): 919 - 926. DOI: 10.2118/15442-PA.

Law, D.-S., Yang, Z.-M., Stone, T. 1992. Effect of the presence of oil on foam performance: a field simulation study. *SPERE* **7** (02): 228-236. DOI: 10.2118/18421-PA.

Ma, K., Farajzadeh, R., Lopez-Salinas, J. L., Miller, C. A., Biswal, S. L., Hirasaki, G. J. 2014. Non-uniqueness, numerical artifacts, and parameter sensitivity in simulating steady-state and transient foam flow through porous media. *Transport in porous media* **102** (3): 325-348. DOI: 10.1007/s11242-014-0276-9.

Ma, K., Lopez-Salinas, J. L., Puerto, M. C., Miller, C. A., Biswal, S. L., Hirasaki, G. J. 2013. Estimation of Parameters for the Simulation of Foam Flow through Porous Media. Part 1: The Dry-Out Effect. *Energy & Fuels* **27** (5): 2363-2375. DOI: 10.1021/ef302036s.

Mannhardt, K., Novosad, J. J., Schramm, L. L. 1996. Core flood evaluation of hydrocarbon solvent foams. *JPSE* **14** (3): 183-195. DOI: 10.1016/0920-4105(95)00046-1.

Peng, D.-Y., Robinson, D. B. 1976. A new two-constant equation of state. *Ind. Eng. Chem. Fundam* **15** (1): 59-64

Romero, L., Ziritt, J., Marin, A., Rojas, F., Mogollón, J., Paz, E. M. F. 1996. Plugging of high permeability-fractured zones using emulsions. Paper presented at SPE/DOE Improved Oil Recovery Symposium, 21-24 April, Tulsa, USA. DOI: 10.2118/35461-MS.

Rossen, W. R., Wang, M. W. 1999. Modeling Foams for Acid Diversion. *SPEJ* **4** (02): 92 - 100. 10.2118/56396-PA.

Schramm, L. L. 1994. Foam sensitivity to crude oil in porous media. *Advances in Chemistry Series* **242**: 165-165

Suffridge, F. E., Raterman, K. T., Russell, G. C. 1989. Foam Performance Under Reservoir Conditions. Paper presented at SPE Annual Technical Conference and Exhibition, 8-11 October,, San Antonio, USA. DIO: 10.2118/SPE-19691-MS.

Verlaan, M., Boerrigter, P. M. 2006. Miscible Gas-Oil Gravity Drainage. Paper presented at International Oil Conference and Exhibition in Mexico, 31 August-2 September, Cancun, Mexico. DOI: 10.2118/103990-MS.

Xiao, C., Balasubramanian, S. N., Clapp, L. W. 2016. Rheology of Supercritical CO2 Foam Stabilized by Nanoparticles. Paper presented at SPE Improved Oil Recovery Conference, 11-13 April, Tulsa, Oklahoma, USA. DOI: 10.2118/179621-MS.

Yang, S. H., Reed, R. L. 1989. Mobility Control Using CO2 Forms. Paper presented at SPE Annual Technical Conference and Exhibition, 8-11 October, , San Antonio, Texas. DOI: 10.2118/19689-MS.

Yu, J., An, C., Mo, D., Liu, N., Lee, R. L. 2012. Foam Mobility Control for Nanoparticle-Stabilized Supercritical CO2 Foam. Paper presented at SPE Improved Oil Recovery Symposium, 14-18 April, Tulsa, Oklahoma, USA. DOI: 10.2118/153336-MS.

Zeng, Y., Farajzadeh, R., Eftekhari, A. A., Vincent-Bonnieu, S., Muthuswamy, A., Rossen, W. R., Hirasaki, G. J., Biswal, S. L. 2016. Role of Gas Type on Foam Transport in Porous Media. *Langmuir* **32** (25): 6239-6245. DOI: 10.1021/acs.langmuir.6b00949.